ROF for the Combined Field Integral Equation

Hua-Long Sun[1, *], Chuang Ming Tong[1], Qi Liu[2], and Gao Xiang Zou[1]

Abstract—This article proposes a computational scheme for a combined field integral equation to compute electromagnetic scattering, which is Reduced order Fitting Green's function's Gradient and Fitting Green's function with Fast Fourier Transform (ROF). This new scheme can greatly reduce computation time compared to integral equation Fast Fourier Transform (IE), as well as Fitting Green's function's Gradient and Fitting Green's function with Fast Fourier Transform (FGG). Firstly, based on the property of Green's functions' integral under special condition, real-coefficient fitting method is utilized to replace the original complex values expression of combination coefficients with the real values. Secondly, a cross-shaped grid named as reduced order grid is presented to reduce computation time for modified near-field coupling impedance. Thirdly, by combining real-coefficient fitting method and reduced order grid, a new scheme of ROF is achieved. Finally, some examples verify ROF, which has advantages, such as higher efficiency than that of IE based on original grid and FGG based on cross-shaped grid, being not sensitive to grid spacing, and keeping the same precision as that of IE based on original grid.

1. INTRODUCTION

The method of moments (MOM) [1] is one of the typical numerical algorithms based on partitioning the IE with triangles as surface elements where vector basis functions are defined to transform the integral equation into a matrix equation. Focusing on accelerating matrix-vector products of MOM's resultant matrix equation, there are two kinds of methods: those related to the fast multipole method (FMM) [2, 3] and multilevel fast multipole algorithm (MLFMA) [4] based on addition theorem [5, 6], and those based on FFT that relies on decoupling the source points and field points to make resultant matrix sparse, using FFT to accelerate resultant matrix-vector products [7–9]. Compared to the former kind of methods, FFT-based methods are more suitable for the case of dense meshing [10]. When solving multiscale problem, Kong et al. [10] have given a meaningful attempt to propose a combined scheme of these two kinds of methods. Among the latter methods, Integral Equation with FFT (IE) [9] projects Green's function on Cartesian Grid nodes by Lagrange interpolation; however, computation precision is not high. Aiming at improving precision, Fitting Green's function's Gradient and Fitting Green's function with FFT (FGG) [11] is proposed utilizing fitting method, whose coefficients are expressed by complex values [12]. For transforming complex fitting coefficients into real coefficients, the authors proposed real-coefficient fitting method [12], which can reduce half storage requirement of fitting coefficient and accelerate solving process. Usually, all of FFT-based algorithms need a cube-like grid enclosing source/field points, so that basis functions or Green's functions can be expressed by the linear combination of the ones on this cube-like grid. After dividing computation domain into two parts of near- and far-field couplings, in which the part of far-field coupling can be accelerated by FFT, and the part of near-field coupling must be computed directly. It is noticeable that if the grids of source

and field points have common grid nodes, near-field coupling impedance elements need to be modified to avoid the singularity of Green's function, and mass modified computations based on the original grid costs a great deal of computation time.

In this article, ROF has been proposed. Firstly, new fitting method or real-coefficient fitting method is used to compute purely real combination coefficients, which can reduce half of the storage requirement for combination coefficients and resultant sparse matrices, and accelerate iteration process compared to original fitting method in FGG. Secondly, reduced order grid or the cross-shaped grid different from original grid is proposed to reduce the modified products' number concerning near-field coupling impedances. Reduced order grid is very suitable for fitting method [11, 12] rather than Lagrange interpolation in IE due to low precision of the interpolation method. Thirdly, by combining new fitting method and reduced order grid, a new scheme of ROF is presented. At last, for verifying ROF, some examples are given to compare ROF, IE based on original grid and FGG based on reduced order grid, which shows that ROF has less pre-computation time, higher efficiency than IE based on original grid and FGG with reduced order grid, and ROF is almost not sensitive to grid spacing and keeps the same precision as one of IE with original grid.

2. FORMULATIONS

2.1. Real-Coefficient Fitting Method Used in FGG

The unknown equivalent electric current distribution on the conductor's surface can be achieved by solving electric field integral equation (EFIE) and magnetic field integral equation (MFIE) [1]:

$$4\pi \mathbf{E}^{inc}|_t = [jk_0\eta_0 \int_S [g(\mathbf{r}, \mathbf{r}')\mathbf{J}(\mathbf{r}) + (1/k_0^2)\nabla g(\mathbf{r}, \mathbf{r}')\nabla' \cdot \mathbf{J}(\mathbf{r}')]ds']|_t,$$

$$4\pi \mathrm{H}^{inc}|_t = [2\pi(\hat{n} \times \mathbf{J}(\mathbf{r})) + \mathrm{P.V.} \int_S \mathbf{J}(\mathbf{r}') \times \nabla gds']|_t, \qquad (1)$$

where $\mathbf{E}^{inc}$ and $\mathbf{H}^{inc}$ are the incident electric and magnetic fields, respectively; $\mathbf{J}(\mathbf{r})$ is the equivalent electric current; η_0 and k_0 are the wave impedance and the wave number in the free space; P.V. is the principal value integral; $g(\mathbf{r}, \mathbf{r}')$ is the Green's function in the free space with the form of $g(\mathbf{r}, \mathbf{r}') = e^{(-jk_0|\mathbf{r}-\mathbf{r}'|)}/|\mathbf{r} - \mathbf{r}'|$; subscript t denotes the tangent part; $\hat{n}$ is the unit outer normal vector on the object's surface. Then choose RWG [13] functions as the basis functions and testing functions to formulate resultant matrix equation:

$$[aZ^{\mathrm{EFIE}} + (1-a)Z^{\mathrm{MFIE}}]I = V \qquad (2)$$

with a being the combination coefficient satisfying $0 \leq a \leq 1$, whose impedance elements have the form of:

$$Z_{mn}^{\mathrm{EFIE}} = jk_0\eta_0 \int_{T_m} ds\mathbf{f}_m(\mathbf{r}) \cdot \int_{T_n} g(\mathbf{r}, \mathbf{r}')\mathbf{f}_n(\mathbf{r}')ds' - \frac{j\eta_0}{k_0} \int_{T_m} ds\nabla \cdot \mathbf{f}_m(\mathbf{r}) \int_{T_n} g(\mathbf{r}, \mathbf{r}')\nabla' \cdot \mathbf{f}_n(\mathbf{r}')ds',$$

$$Z_{mn}^{\mathrm{MFIE}} = 2\pi \int_{T_m} \mathbf{f}_m(\mathbf{r}) \cdot \mathbf{f}_n(\mathbf{r})ds + \int_{T_m} ds[\hat{n} \times \mathbf{f}_m(\mathbf{r})] \cdot \int_{T_n} \nabla g(\mathbf{r}, \mathbf{r}') \times \mathbf{f}_n(\mathbf{r}')ds', \qquad (3)$$

in which T_m and T_n are the triangular patches of $\mathbf{f}_m(\mathbf{r})$ and $\mathbf{f}_n(\mathbf{r})$, respectively. According to the interaction between basis functions, resultant impedance matrix can be split into two parts of near-field interaction and far-field interaction [12]:

$$aZ^{\mathrm{EFIE}} + (1-a)Z^{\mathrm{MFIE}} \approx [a(Z_{\mathrm{MOM}}^{\mathrm{EFIE\text{-}near}} - Z_{\mathrm{FFT}}^{\mathrm{EFIE\text{-}near}}) + (1-a)(Z_{\mathrm{MOM}}^{\mathrm{MFIE\text{-}near}} - Z_{\mathrm{FFT}}^{\mathrm{MFIE\text{-}near}})]$$
$$+ aZ_{\mathrm{FFT}}^{\mathrm{EFIE\text{-}total}} + (1-a)Z_{\mathrm{FFT}}^{\mathrm{MFIE\text{-}total}}. \qquad (4)$$

As we know, if the distance between basis functions is less than near zone boundary d_{near}, near-field interaction impedances computed by FFT-based algorithms present poor accuracy, so all of the FFT-based algorithms need the pre-correction of near-field interaction impedances. In Eq. (4), $Z_{\mathrm{MOM}}^{\mathrm{EFIE\text{-}near}} - Z_{\mathrm{FFT}}^{\mathrm{EFIE\text{-}near}}$ and $Z_{\mathrm{MOM}}^{\mathrm{MFIE\text{-}near}} - Z_{\mathrm{FFT}}^{\mathrm{MFIE\text{-}near}}$ are pre-corrected matrices, in which the subscript

MOM stands for being computed by MOM, and subscript FFT stands for being computed by FFT-based algorithm. $Z_{\text{FFT}}^{\text{EFIE}}$ and $Z_{\text{FFT}}^{\text{MFIE}}$ have the expressions of:

$$Z_{\text{FFT}}^{\text{EFIE}} = jk_0\eta_0\mathbf{\Pi} \cdot G\mathbf{\Pi}^T - j(\eta_0/k_0)\Pi_d G\Pi_d^T, \quad Z_{\text{FFT}}^{\text{MFIE}} = \mathbf{\Pi}_g \cdot (\nabla G \times \mathbf{\Pi}^T), \tag{5}$$

where $\mathbf{\Pi}$, Π_d and $\mathbf{\Pi}_g$ are sparse matrices with the expression similar to Eqs. (10)–(11) in [17], composed of basis functions and fitting coefficients. G stands for a triple Toeplitz matrix on Cartesian grid nodes. Superscript T identifies transpose operator. After substituting Eqs. (3)–(5) into Eq. (2), matrix-vector products in Eq. (2) per iteration can be accelerated by FFT. Each iteration needs 11 FFTs, and the whole computation complexity is reduced from $O(N^2)$ to $O(N^{1.5}\log N)$ [11].

Similar to other FFT-based methods, FGG also needs fitting cube C_m composed of $N_C = (M+1)^3$ grid nodes with the center being c_m in which M is expansion order. Fig. 1 shows the case of $M = 2$. Grid spacing is h in three coordinate directions. Suppose r_m to be the minimum radius of spherical surface enclosing C_m. R_m is the radius of testing spherical surface S_m with the same center c_m. Assume $R_m = r_m + 0.05\lambda$, λ is the wavelength in free space. $\{\mathbf{r}_t\}_1^{T_e}$ are testing points located on S_m, which are chosen according to [12]. So Green's function and its gradient can be expressed as:

$$g(\mathbf{r}, \mathbf{r}') = \sum_{u \in Cm} \pi_{u,Cm}^{\mathbf{r}} g(\mathbf{r}_u, \mathbf{r}'), \quad \nabla g(\mathbf{r}, \mathbf{r}') = \sum_{u \in Cm} \pi_{u,Cm}^{\mathbf{r}} \nabla g(\mathbf{r}_u, \mathbf{r}') \tag{6}$$

where $\{\pi_{u,Cm}^{\mathbf{r}}\}_{u=1}^{Nc}$ are the fitting coefficients. In this paper, both FGG and ROF employ direct inheriting scheme for fitting the gradient which features easy formulation [11]. $\mathbf{r}$ and $\mathbf{r}'$ are the position vector of field and source points, respectively. $\mathbf{r}$ is surrounded by C_m, and $\mathbf{r}_u$ is the grid node's vector. For solving fitting coefficients, we assume $\mathbf{r}' = \mathbf{r}_t$, and over determinant fitting matrix equation with the dimension of $T_e \times N_C$ can be formulated as:

$$[X]\{\pi_{Cm}^{\mathbf{r}}\} = [Y], \quad \{\pi_{Cm}^{\mathbf{r}}\} = [X]^+[Y],$$
$$X_{i,j} = g(\mathbf{r}_j, \mathbf{r}_{ti}), \quad i \in [1, T_e], \quad j \in [1, N_C], \tag{7}$$
$$Y_i = g(\mathbf{r}, \mathbf{r}_{ti}), \quad i \in [1, T_e],$$

in which $[X]^+$ denotes the generalized inverse of $[X]$; fitting coefficients $\{\pi_{u,Cm}^{\mathbf{r}}\}_{u=1}^{Nc}$ are determined by solving this fitting matrix equation, so sparse matrices $\mathbf{\Pi}$, Π_d and $\mathbf{\Pi}_g$ can be decided.
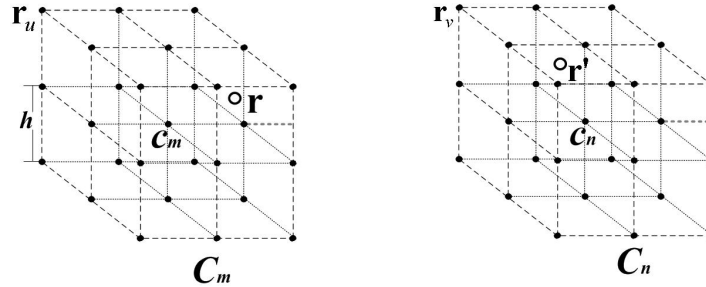
Figure 1. Illustration of representing Green's function and its Gradient within Cartesian grid.

The most time-consuming per iteration is matrix-vector multiplications concerning sparse matrices composed of fitting coefficients and basis functions. Noticeably, fitting coefficients by Adaptive Integral Method [7] and IE are real values, and the fitting coefficients by pre-corrected-FFT [8] and FGG are complex values, so Adaptive Integral Method and IE have higher efficiency and lower accuracy than pre-corrected-FFT and FGG under the same grid spacing and expansion order. In essence, fitting technique in pre-corrected-FFT and FGG is near-matching [14]. When testing points $\{\mathbf{r}_t\}_1^{T_e}$ on the testing spherical surface obey the mean distribution, they have equal weight $w_t = 4\pi R_m^2/T_e$, which is the area of small cell on testing spherical surface. Obviously, $[X]^+$ can be expressed as $[X]^+ = [w_t X^H X]^+[w_t X^H]$.

Furthermore, taking the limit as the number of testing points $T_e \to \infty$ [12], we can rewrite Eq. (7) with the expression of

$$\{\pi_{Cm}^{\mathbf{r}}\} = [A]^+[B],$$

$$A_{i,j} = \int_{S_m} g^*(\mathbf{r}_i, \mathbf{r}_t)g(\mathbf{r}_j, \mathbf{r}_t)dS, \quad i,j \in [1, N_C], \tag{8}$$

$$B_i = \int_{S_m} g^*(\mathbf{r}_i, \mathbf{r}_t)g(\mathbf{r}, \mathbf{r}_t)dS, \quad i \in [1, N_C].$$

Then, $g(\mathbf{r}_i, \mathbf{r}_t)$ and $g(\mathbf{r}_j, \mathbf{r}_t)$ can be expanded by the addition theorem. $\{\hat{k}_p\}_1^{K_1}$ and $\{\hat{k}_q\}_1^{K_2}$ with the total number $K_1 = 2L_1^2$ and $K_2 = 2L_2^2$ are the angular directions on Ewald sphere, in which both satisfy the symmetry to the center of Ewald sphere [12]. K_1 and K_2 are relative to $g(\mathbf{r}_i, \mathbf{r}_t)$ and $g(\mathbf{r}_j, \mathbf{r}_t)$, respectively. So $A_{i,j}$ has the approximation $\bar{A}_{i,j}$ satisfying

$$\bar{A}_{i,j} = [(k_0 r_t)^2/2\pi] \sum_{p=1}^{K_1/2} \sum_{q=1}^{K_2} \omega_p \omega_q \cos(\mathbf{k}_p \cdot \mathbf{r}_i - \mathbf{k}_q \cdot \mathbf{r}_j) \sum_{l_1=0}^{L} (2l_1 + 1) \left| h_{l_1}^{(2)}(k_0 r_t) \right|^2 P_{l_1}(\hat{k}_p \cdot \hat{k}_q). \tag{9}$$

where $h_{l_1}^{(2)}$ is the 2nd kind spherical Hankel function of order l_1; P_{l_1} is the Legendre function of order l_1; ω_p and ω_q are the Gauss weights, $L = \min\{L_1, L_2\}$. When $K = \max\{K_1, K_2\} \to \infty$,

$$A_{i,j} = \lim_{K \to \infty} \bar{A}_{i,j}. \tag{10}$$

Besides, B_i has a similar expression to $A_{i,j}$. As we can see, $A_{i,j}$ and B_i are purely real when the test points approximate infinite on testing spherical surface. The detailed deduction can be referred to [12]. We can use $\bar{A}_{i,j}$ and $\bar{B}_i$ to approximate $A_{i,j}$ and B_i, and the fitting coefficients are real values.
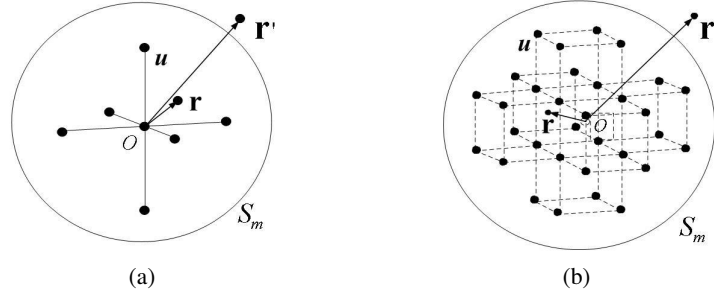
2.2. Reduced Order Grid with the Cross shape

As shown in Fig. 1, the original grid is a cube composed of $(M + 1)$ grid nodes in each Cartesian coordinate direction. When two grids of source and field points are close enough to have not less than one common grid nodes, it will result in the singularity of Green's functions and their gradients. So these impedance elements with fitting grids having the common grid nodes need to be modified by traditional MOM, which is named as near-field coupling modification shown below:

$$Z_{m,n}^{\mathrm{modified}} = Z_{m,n}^{\mathrm{MOM}} - \sum_{\substack{\mathbf{r}_u \in C_m \\ \mathbf{r}_v \in C_n \\ u \neq v}} \left\{ a \left[jk_0\eta_0 \mathbf{\Pi}_u \cdot \mathbf{\Pi}_v - j\frac{\eta_0}{k_0}\Pi_{d,u}\Pi_{d,v} \right] g(\mathbf{r}_u, \mathbf{r}_v) + (1-a)\mathbf{\Pi}_{g,u} \cdot (\nabla g(\mathbf{r}_u, \mathbf{r}_v) \times \mathbf{\Pi}_v) \right\},$$

$$\tag{11}$$

with $\mathbf{\Pi}_i$, $\Pi_{d,i}$ and $\mathbf{\Pi}_{g,i}$ being the elements of sparse matrices. When adopting the original grid, the modified products' number concerning each near field coupling impedance is $[(M+1)^6 - (M+1)^3] \leq N_M \leq [(M+1)^6 - 1]$, in which N_M is the number of series' terms at the right hand in Eq. (11). This process occupies mass pre-computation time and limits the total computation efficiency.

This article proposes a reduced order grid with the cross shape shown in Fig. 2. Fig. 2(a) belongs to expansion order $M = 2$, and that grid has 7 grid nodes, which is less than the 27 grid nodes in original grid. Fig. 2(b) belongs to expansion order $M = 3$, and that grid has 32 grid nodes, which is less than the 64 grid nodes in original grid. Obviously, computation time for modified products based on the reduced order grid is greatly less than that based on the original grid. This new grid is named as reduced order grid. It is assumed that only one basis function exists within C_m, that one test function exists within C_n, and that one point Gaussian integral formula is adopted onto basis and test functions' triangular patches. Table 1 shows the comparison of these two kinds of grids in the number of each impedance's modified products. We can see that the maximum of modified terms in reduced order grid is less than 25% of that in original grid. As a result, pre-computation time can be greatly reduced, and computation efficiency will be improved.

Specially, if a reduced order grid is used in Lagrange interpolation to compute combination coefficients, computation precision is not satisfied. So this paper adopts fitting method for reduced order

(a) (b)

Figure 2. Illustration of reduced order grid with the cross shape, (a) expansion order $M = 2$ with 7 grid nodes, (b) $M = 3$ with 32 grid nodes.

Table 1. Comparison of two kinds of grids.

	Expansion order	Number of grid nodes	Maximum of modified terms per C_m
Reduced order grid	2	7	36
	3	32	961
Original grid	2	27	676
	3	64	3969

grid, which can guarantee computation precision. However, combination coefficients with fitting method are usually complex values, which results in increasing computation time. If combination coefficients can be expressed with real values, computation time and storage requirement for combination coefficients will be reduced by one half, and computation efficiency will be improved. This assumption can be realized by new fitting method introduced in the following section.

It is worth to note that the truncated Green's function in $[A]^+$ and $[B]$ of Eq. (8) has some common terms for all of fitted points. $[A]^+$ can be computed once since it only concerns common grid cube. And $[B]$ needs to be computed for the different fitted points except for the common terms. So the complexity of computing fitting coefficients does not consume extra computation time.

2.3. New Scheme of ROF

New fitting method is introduced below:

1). According to fitting matrix Eq. (8), substitute $A_{i,j}$ and B_i by their approximations $\bar{A}_{i,j}$ and $\bar{B}_i$. $\bar{A}_{i,j}$ and $\bar{B}_i$ have expressions similar to Eq. (9).
2). Solve Eq. (8) to achieve purely real fitting coefficients.

For comparing new fitting method based on reduced order grid, one example of reduced order grid with expansion order $M = 2$ is shown in Fig. 3. Grid spacing satisfies $h = 0.2\lambda$ (λ is wavelength in free space), and a fixed point is located outside this reduced order grid for source point $\mathbf{r}'(0, 0, (M + 1)h)$, whose position is right at the near-field coupling boundary $d_{\text{near}} = (M + 1)h$. The fitted point is set to move along with the line ($x = y = z$) from its center to the point of ($0.5h$, $0.5h$, $0.5h$). The original fitting method is based on reduced order grid, and Lagrange interpolation in IE is based on original grid. For the new fitting method, we can set $L_1 = L_2 = 14$, $K_1 = K_2 = 392$, which are decided by truncated Green's function having the number of modes $L = kd + 5\ln(\pi + kd)$ with $d = \sqrt{3}Mh$. The original fitting method is actually Least-Square Method (LSM) [11], and test points obey mean distribution on the testing spherical surface with the number of $T_e = 392$. We also give the result of new fitting method based on original grid. Then the relative error of Green's function is defined as RE(g) with the
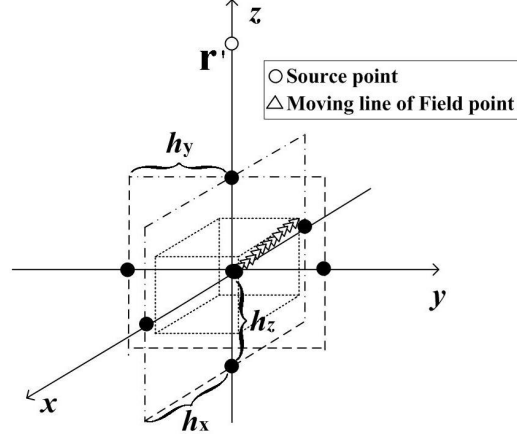
Figure 3. Reduced order grid of expansion order $M = 2$ with 7 grid nodes and the relative position between fixed point $\mathbf{r}' = (0, 0, 3h)$ and the moving field point along with the line.
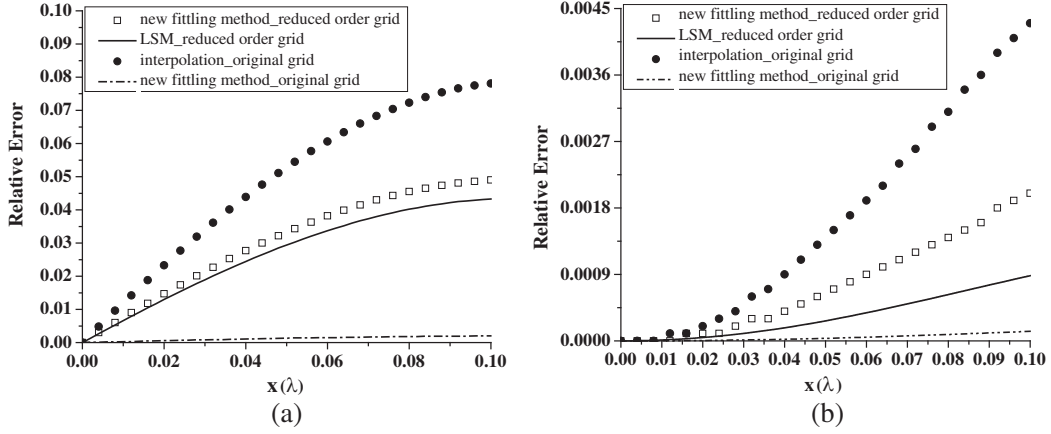
Figure 4. Relative error curves of different methods based on different grids, (a) is for the fitted point being along with the diagonal line; (b) is for the fitting point being along with x axis.

expression of

$$\text{RE}(g) = \frac{\left| g(\mathbf{r}, \mathbf{r}') - \sum_{u=1}^{(M+1)^3} \pi_{u,Cm}^{r} g(\mathbf{r}_u, \mathbf{r}') \right|}{|g(\mathbf{r}, \mathbf{r}')|}, \tag{12}$$

which reflects different methods' precision to approximate the original Green's function. In Eq. (12), N equals 7 in new fitting method and LSM, 27 in Lagrange interpolation. Relative error curves are shown in Fig. 4(a). As we can see, new fitting method and LSM based on reduced order grid have higher precision than Lagrange interpolation based on original grid, and the new fitting method has comparable precision with LSM. The result of the new fitting method based on reduced order grid has lower precision than that based on original grid, since reduced order grid has less grid nodes than original grid. When the fitted point moves along with x axis from its center to the point of $(0.5h, 0, 0)$, the result shown in Fig. 4(b) is similar to that in Fig. 4(a), and the curve in Fig. 4(b) also monotonically increases with the distance.

Subsequently, by combining new fitting method and reduced order grid, ROF for combined field integral equation is achieved to compute electromagnetic scattering problem. Similar to original fitting method, new fitting method only concerns Green's function. Importantly, new scheme greatly

reduces computation time of near-field coupling modification due to reduced order grid. Regardless of computation efficiency, computation precision of the new scheme is lower than that of FGG based on original grid, which can be improved by increasing expansion order or decreasing grid spacing.

3. NUMERICAL RESULTS AND DISCUSSION

This section gives several examples to demonstrate efficiency and precision of ROF. The principle of choosing its grid for fitted point is that the distance from the grid's center to the fitted point is not more than $0.5h$ in each coordinate direction.

In order to accelerate the convergence for solving Eq. (2), an iteration solver of BiCGSTAB [15] is adopted, and a high efficiency FFTW [16] library of OpenMP version is employed for parallel computing FFTs in each iteration. The computing platform is AMD processor of 2.3 GHz with 64 kernel and 64 GB RAM.

ROF and FGG are based on reduced order grid, whereas IE is based on original grid. ROF adopts the new fitting method. FGG adopts original fitting method or LSM. IE adopts Lagrange interpolation.

3.1. A PEC Sphere

A PEC sphere with radius of 6λ is discretized by triangular patches, including 97864 unknowns. Set expansion order $M = 2$ with 7 grid nodes. When grid spacing satisfies $h = 0.1\lambda$, 0.2λ, the truncation number of infinite series in ROF satisfies $L = 10$, 14, and the number of test points in FGG satisfies $T_e = 200$, 392. Fig. 5 shows the bistatic RCS curves computed by ROF, FGG and IE, respectively. It is worth to note that when adopting IE, combination coefficients of $\nabla g(\mathbf{r}, \mathbf{r}')$ are the same as those of $g(\mathbf{r}, \mathbf{r}')$ [17]. For comparing accuracy of three schemes, the root of mean square error (RMSE) [12] is defined for comparison (N is the number of unknowns of the recorded zenith).

$$RMSE = \sqrt{\frac{1}{N} \sum_{m=1}^{N} \left| (RCS/\lambda^2)^{Calculated} - (RCS/\lambda^2)^{MOM} \right|^2}. \tag{13}$$
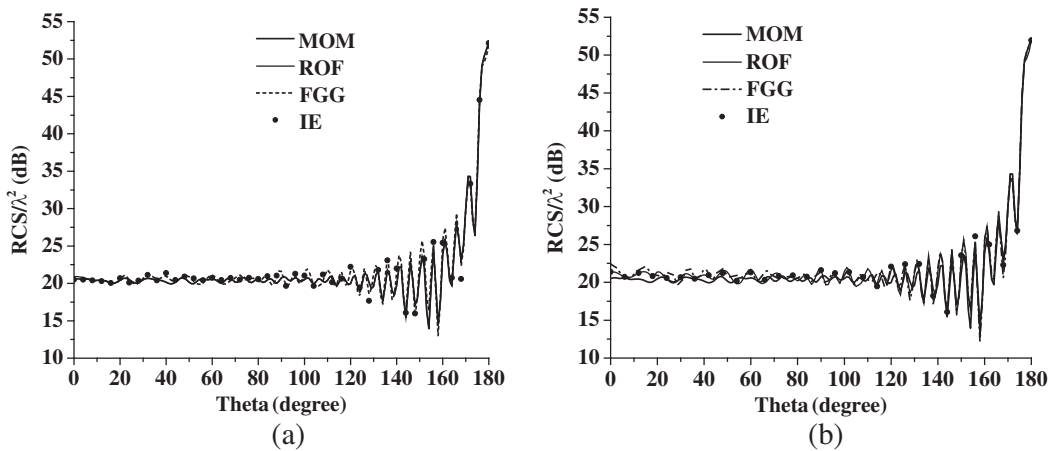
Figure 5. Comparison of three schemes with (a) $h = 0.1\lambda$ and (b) $h = 0.2\lambda$.

Table 2 shows that due to reduced order grid, ROF reduces storage by 67%, improves efficiency by almost 60% compared to IE, and due to real coefficients computed by new fitting method, the new scheme only needs half of storage, 34% total consuming time compared to FGG. Due to adopting reduced order grid in ROF and FGG compared to original grid in IE, they have less total memory, memory of sparse coefficients matrices, pre-computation time and time per iteration than ones of IE. And due to adopting real coefficient scheme in ROF, it has less total memory, memory of sparse coefficients matrices and

Table 2. Comparison of three schemes.

| Grid spacing h/λ		Memory of sparse coefficients matrices/MB	Total memory requirement/MB	Pre-computation time(s)	Time per iteration(s)	Total time(s)	RMSE
0.1	ROF	82.12	875.6	422	42	758	0.10
	FGG	164.05	1012.4	427	62.9	1065	0.10
	IE	251.90	2124.3	687.5	102.8	2024	0.11
0.2	ROF	82.15	624.1	209	27.9	432	0.93
	FGG	164.04	866.8	218	39.6	653	0.93
	IE	251.86	1624.5	457	55.7	1125	0.98

time per iteration than ones in FGG. Simultaneously the new scheme keeps the comparable precision to IE and FGG. Therefore, the new scheme can balance reducing computation time and precision. Also, this example gives a fact that the performance of modified near-field coupling directly influences the total computation efficiency, and computing method of combination coefficients directly influences computation precision.

3.2. A PEC Dihedral

This example is a dihedral with angle of 90° shown in Fig. 6. Each plate has a dimension of $5\lambda \times 5\lambda$. The number of unknowns is 9042. The direction and polarization of incident plane wave are also given in Fig. 7.

Grid spacing is set to $h = 0.15\lambda$. Then RCS curves in xoy-plane are given in Fig. 7 with expansion order $M = 2, 3$. The truncation number of the infinite series in ROF can be chosen as $L = 12$ and 17, respectively. The number of test points in FGG can be chosen as $T_e = 288$ and 578 respectively. When expansion order increases, precision of three schemes is improved. ROF and FGG have almost the same precision.

Furthermore, reduced order grid has fewer grid nodes, which results in reduction of near-field coupling modification. Of course, reduced order grid has so few grid nodes that Lagrange interpolation is not suitable. As we can see in Fig. 7, IE with Lagrange interpolation needs more points than the former two schemes to keep higher precision.
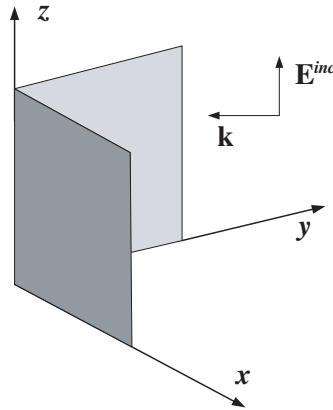
Figure 6. A PEC dihedral with angle of 90° ($\varphi^{\mathrm{in}} = 45°$, $\theta^{\mathrm{in}} = 90°$, $\theta^{\mathrm{S}} = 90°$).
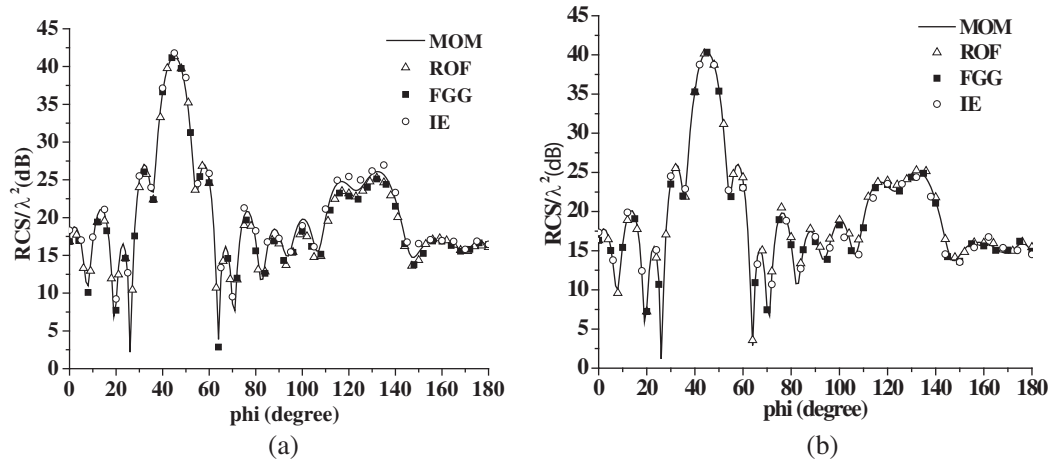
Figure 7. Bistatic RCS curves of ROF, FGG and IE, (a) expansion order $M = 2$; (b) expansion order $M = 3$.

The above examples verify ROF in computation efficiency and precision. The new fitting method of ROF can enhance computation efficiency greatly without degrading precision [11]. The reduced order grid of ROF reduces computation time in modified impedance for improving computation efficiency. It is worth to note that the precision of ROF can satisfy the practical requirement. Furthermore, similar to FGG, ROF only projects the original Green's function onto the nodes of the reduced order grid, and the ultimate computation error mainly comes from the fitting method. The independence of basis functions makes ROF applicable to compute scattering from complex dielectric body by combining surface or volume integral equation [18].

4. CONCLUSION

This paper proposes a new scheme of ROF for the combined field integral equation to compute electromagnetic scattering problems. At first, an important property of Green's function integral is used to formulate a new fitting method, which results in real combination coefficients for decreasing pre-computation time and improving efficient. Next, aiming at reducing computation time of near-field coupling modification, reduced order grid is presented to greatly reduce computation time of near-field coupling modification compared to original grid. In the following, combining reduced order grid and the new fitting method, ROF is achieved which features that the efficiency is higher than that of FGG by LSM in reduced order grid and IE by Lagrange interpolation in original grid; the precision is comparable with that of IE in original grid. Finally, some examples are given for validating new scheme in efficiency and precision. Besides, reduced order grid and the new fitting method can be used in other FFT-based algorithms to reduce computation time of near-field coupling modification and keep high precision.

REFERENCES

1. Harrington, R. F., *Field Computation by Moment Methods*, Oxford University Press Oxford, England, 1996.
2. Engheta, N., W. D. Murthy, V. Rokhlin, and M. S. Vassiliou, "The fast multipole method (FMM) for electromagnetic scattering problems," *IEEE Trans. Antennas Propag.*, Vol. 40, No. 6, 634–641, Jun. 1992.

3. Coifman, R., V. Rokhlin, and S. Wandzura, "The fast multipole method for the wave equation: A pedestrian prescription," *IEEE Antennas Propag. Magn.*, Vol. 35, No. 3, 7–12, Jun. 1993.

4. Song, J., C. C. Lu, and W. C. Chew, "Multilevel fast multipole algorithm for electromagnetic scattering by large complex objects," *IEEE Trans. Antennas Propag.*, Vol. 45, No. 10, 1488–1493, Oct. 1997.

5. Chew, W. C., J. M. Jin, E. Michielssen, and J. M. Song, *Fast and Efficient Algorithms in Computational Electromagnetics*, Artech House, Boston, 2001.

6. Jiang, L.-J. and W. C. Chew, "A mixed-form fast multipole algorithm," *IEEE Trans. Antennas Propag.*, Vol. 53, No. 12, 4145–4156, Dec. 2005.

7. Bleszynski, M., E. Bleszynski, and T. Jaroszewicz, "AIM: Adaptive integral method for solving large-scale electromagnetic scattering and radiation problems," *Radio Sci.*, Vol. 31, No. 5, 1225–1251, Sep.–Oct. 1996.

8. Nie, X. C., L. W. Li, N. Yuan, T. S. Yeo, and Y. B. Gan, "Precorrected-FFT algorithm for solving combined field integral equations in electromagnetic scattering," *Journal of Electromagnetic Waves and Applications*, Vol. 16, No. 8, 1171–1187, Jan. 2002.

9. Mo, S. S. and J.-F. Lee, "A fast IE-FFT algorithm for solving PEC scattering problems," *IEEE Trans. Magn.*, Vol. 41, No. 5, 1476–1479, May 2005.

10. Kong, W. B., H. X. Zhou, K. L. Zheng, and W. Hong, "Analysis of multiscale problems using the MLFMA With the assistance of the FFT-based method," *IEEE Trans. Antennas Propag.*, Vol. 63, No. 9, 4184-4188, Sep. 2015.

11. Xie, J. Y., H. X. Zhou, W. Hong, W. D. Li, and G. Hua, "A highly accurate FGG-FG-FFT for the combined field integral equation," *IEEE Trans. Antennas Propag.*, Vol. 61, No. 9, 4641–4652, Sep. 2013.

12. Sun, H.-L., C. M. Tong, P. Peng, G. X. Zou, and G. L. Tian, "Real-coefficient FGG-FG-FFT for the combined field integral equation," *Progress In Electromagnetics Research M*, Vol. 54, 19–27, 2017.

13. Rao, S. M., D. Wilton, and A. W. Glisson, "Electromagnetic scattering by surfaces of arbitrary shape," *IEEE Trans. Antennas Propag.*, Vol. 30, 409–418, May 1982.

14. Yang, K. and A. E. Yilmaz, "Comparison of pre-corrected FFT/adaptive integral method matching schemes," *Microw. and Opt. Tech. Lett.*, Vol. 53, No. 6, 1368–1372, Jun. 2011.

15. Saad, Y., *Iterative Methods for Sparse Linear Systems*, PWS Publishing Company, Boston, 1996.

16. Frigo, M. and S. Johnson, "FFTW manual," [Online]. Available from: http://www.fftw.org/.

17. Xie, J. Y., H. X. Zhou, W. D. Li, and W. Hong, "IE-FFT for the combined field integral equation applied to electrically large objects," *Microw. and Opt. Tech. Lett.*, Vol. 54, No. 4, 891–896, Apr. 2012.

18. Chen, S.-W., F. Lu, and Y. Ma, "Fitting Green's function FFT acceleration applied to anisotropic dielectric scattering problems," *International Journal of Antennas and Propag.*, Vol. 2, 1–8, Dec. 2015.